

Grasping for a Purpose: Using Task Goals for Efficient Manipulation Planning

Ana Huamán Quispe

Heni Ben Amor

Henrik I. Christensen

M. Stilman†

Abstract—In this paper we propose an approach for efficient grasp selection for manipulation tasks of unknown objects. Even for simple tasks such as pick-and-place, a unique solution is rare to occur. Rather, multiple candidate grasps must be considered and (potentially) tested till a successful, kinematically feasible path is found. To make this process efficient, the grasps should be ordered such that those more likely to succeed are tested first. We propose to use *grasp manipulability* as a metric to prioritize grasps. We present results of simulation experiments which demonstrate the usefulness of our metric. Additionally, we present experiments with our physical robot performing simple manipulation tasks with a small set of different household objects.

I. INTRODUCTION

The ability to grasp objects in order to accomplish a task is one of the hallmarks of human intelligence. Numerous psychological studies show that humans grasp selection depends on the *goal* to be *accomplished* [14]. Decision making during grasping is therefore not only based on stability during manipulation, but also based on task requirements. If a specific grasp does not facilitate the execution of the upcoming sub-tasks, it is omitted from the reasoning process.

In contrast to that, research on robot grasp synthesis has been tilted towards optimizing stability metrics only. A prominent approach is to generate a set of physically stable grasps, one of which is then selected by the high-level planner. If a high-level task planner cannot achieve the goals of the task, it has to back track and try a different grasp. Since no information is flowing between high-level planning and lower-level grasp generation, a large number of grasps may have to be evaluated. If the required grasp is not within the optimized set of candidates, the entire task will fail.

In this paper, we introduce a method for manipulation planning which uses foresight to identify task constraints. Constraints extracted from subsequent sub-tasks are used to synthesize grasps that facilitate overall task completion. Our goal is to derive a fast planning algorithm that can efficiently generate manipulation sequences for *previously unseen* objects. These latter properties, hence, allow a robot to perform manipulation tasks in new environments without resorting to prior 3D models of the object or pre-calculated grasp sets. This ability to generalize is realized by using a super-quadric representation of objects. We show how super-quadrics can be extracted from a single depth image and how they can be used to generate a large set of grasp candidates.

Institute for Robotics and Intelligent Machines, Georgia Institute of Technology, Atlanta, GA 30332, USA. ahuaman3@gatech.edu, hbenamor@cc.gatech.edu, hic@cc.gatech.edu



Fig. 1: Example of grasp selection based on goal constraints: The goal location of the chips box is surrounded by nearby objects, hence an overhead grasp must be selected for manipulation. If not for the obstacles present, a different grasp (overlaid in red) from the side would be easier to execute.

Short planning times are realized by introducing a heuristics that efficiently guides the search by incorporating arm kinematics. Inspired by the *end-comfort effect* [20] in humans, grasps are preferred which lead to a comfortable arm configuration at the end of a task. We borrow ideas from this work and propose to use a metric based on manipulability as a measurement of end-comfort.

The contributions of this paper are threefold, namely (1) a framework for online grasp planning that incorporates future task constraints into the grasp synthesis process, (2) an efficient grasp generation approach based on super-quadrics that works with previously unseen objects, (3) the end-comfort heuristics for efficient search during manipulation planning.

The rest of this paper is organized as follows: Section II present relevant work in the area of grasp synthesis and grasp selection. Section IV presents our grasp generation method using a primitive-based approach and in Section V we introduce our manipulability-based strategies to prioritize the generated grasps. Section VI shows the results of the comparisons in simulation and the metrics we used to compare their performance. Finally, we present the application of our approach in our physical robot. We conclude this paper with section VII, where we provide some discussion regarding future work, and the advantages and shortcomings of our approach.

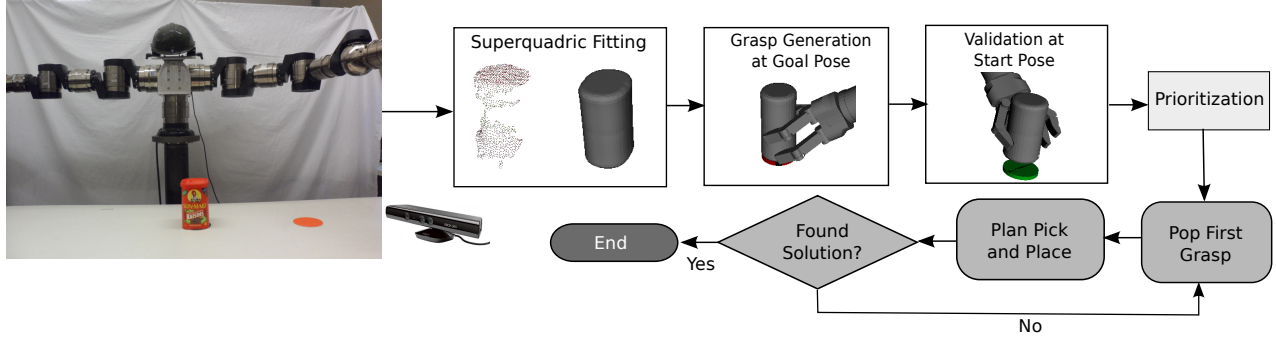


Fig. 2: Manipulation planning pipeline: a partial point cloud of the object is first analyzed for symmetries and then turned into a superquadric representation. Grasps at the goal and the start position are generated and then prioritized according to end-comfort. Potential grasps are then analyzed within the plan and then executed.

II. RELATED WORK

In this section we review work concerning grasp synthesis and grasp selection. For a more detailed review of previous research in the area, we suggest the interested reader to consult the excellent reviews from Bohg [3] and Sahbani [21].

Pioneering work on grasp selection was developed by Cutkosky [5], who observed that humans select grasps in order to satisfy 3 main types of constraints: Hand, object and task-based constraints. As pointed out by Bohg et al. in [3], there is little work on task-dependent grasping when compared to work focused on the first two constraints. Hence, the main goal for a planner is to find a grasp such that the robot can approach the object and execute the said grasp, without further regard of what the robot will do once the object is picked.

Grasp generation methods vary widely depending on the assumptions considered. In the case of grasp planning for known objects, Ciocarlie et al. [4] presented the concept of eigengrasps, which was exploited to generate candidate grasps searching in a low dimensional hand posture space using their GraspIt! simulator. Diankov generated grasps by sampling the surfaces of object meshes and using the normals at the sample points to guide the approach direction of the hand [6]. Approaches using primitive representations were also proposed such that the grasp generation depends on the particular primitive characterization: Miller et al. [15] proposed to use a set of primitive shapes (cylinder, box, ball) to decompose complex objects. Huebner and Kragic [12] used bounding boxes, Przybylski et al. proposed the Medial Axis representation [18], Goldfeder et al. [9] used superquadrics due to their versatility to express different geometry types with only 5 parameters.

In all the cases mentioned, the grasps are generated offline and stored in a database for future use. These grasps are usually ranked based on their force-closure properties, which theoretically express the robustness and stability of a grasp. One of the most popular metrics (ϵ) was proposed by Ferrari and Canny [7]. However, it has been noted by different authors that analytical metrics do not guarantee a stable grasp when executed in a real robot. This can be explained

by the fact that these classical metrics consider assumptions that don't always hold true in real scenarios (dynamics, perceptual and modelling inaccuracies, friction conditions). On the other hand, studies that consider human heuristics to guide grasp search have shown remarkable results, outperforming classical approaches. In [1], Balasubramanian observed that when humans kinesthetically teach a robot how to grasp objects, they strongly tend to align the robotic hand along one of the object's principal axis, which later results in more robust grasps. The author termed *skewness* to the metric measuring the axis deviation. In [19], Przybylski et al. combine the latter metric with ϵ and use it to rank grasps produced with GraspIt!. Berenson et al. [2] proposed a score combining 3 measures: ϵ , object clearance and the robot relative position to the object.

In this work we are interested in manipulation of unknown objects. Multiple approaches of this kind have flourished during the last few years, particularly due to the advent of affordable RGB-Depth sensors. Since the 3D information is partial and noisy, classical approaches to grasp generation cannot be directly used. Rather, most of the current work uses heuristics to guide grasp generation based on local representation of the object geometry features (or global features if the object shape is approximated). In [10], Hsiao et al. use the bounding box of the object segmented pointcloud to calculate grasp approach directions using a set of heuristics. We should notice that for most of these approaches, their effectiveness can only be verified empirically.

As we mentioned at the beginning of this section, the metrics we discussed above do not consider the task to be executed *after* the grasp is achieved. Some authors, however, have investigated this issue at some level. In pioneering work, [13] Li and Sastry proposed the concept of the *task ellipsoid*, which maximizes the forces to be applied in the direction of the task. More recently, Pandey et al. [16] proposed a framework to select a grasp such that the object grasped can be manipulated in a human-robot interaction scenario in which the goal pose of the object is not entirely constrained.

Finally, although one of our main concerns is to select a grasp that is suitable for the task to be executed, we also consider important to use a grasp that allows for a simple, easy

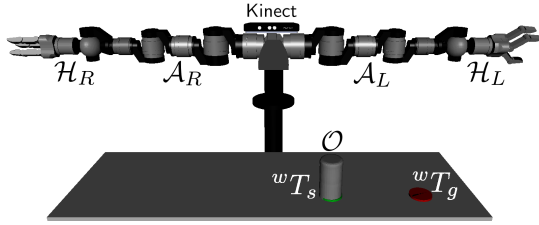


Fig. 3: System setup and problem description.

arm execution. Interestingly, the problem of grasp planning is usually considered isolated from arm planning. In some recent work, Vahrenkamp et al. proposed Grasp-RRT [22] in order to perform both grasp and arm planning combined. In a similar vein, Roa et al. also proposed an approach that solve both problems simultaneously [8]. Both approaches focus on *reaching tasks*. Our approach tackles pick-and-place tasks in which reaching is only the first half of the solution (*object placing* being the second). We make use of our proposed heuristics to solve the complete pick-and-place problem in a manner as efficient as possible by means of grasp prioritization.

III. PROBLEM DEFINITION AND ASSUMPTIONS

Our problem description can be explained as follows: Given a bimanual manipulator \mathcal{R} and a simple object \mathcal{O} , the manipulation task consists on transporting \mathcal{O} from a given start pose wT_s to a final pose wT_g .

Figure 3 depicts the problem described. The following constraints are considered:

- A 3D model of \mathcal{O} is not available beforehand.
- A one-view pointcloud of the scenario is available from the Kinect sensor mounted on top of the robot shoulders.
- Each limb of \mathcal{R} consists of a 7-DOF arm ($\mathcal{A}_L, \mathcal{A}_R$) and a 3-fingered hand ($\mathcal{H}_L, \mathcal{H}_R$). A semi-analytical IK solver is available for \mathcal{A}_L and \mathcal{A}_R .

In the following sections we will describe our basic approach for problems in which only the use of one arm is required to solve the manipulation task described.

IV. GRASP GENERATION FOR UNKNOWN OBJECTS

As our problem description stated, our approach must find a plan such that \mathcal{O} can be grasped at wT_s , transported and finally repositioned at wT_g . Our approach consists on 4 main steps, shown in Figure 2. The first 3 steps (object fitting, grasp generation and grasp validation) will be explained in the rest of this section.

A. Object Representation using Superquadrics

Requiring complete 3D models of objects before grasp synthesis severely limits the application domains of robot manipulation. Modern depth cameras partly solve the problem, since they allow the robot to estimate the surface of an object. Yet, since the point clouds are acquired from a specific perspective, they only hold partial shape information about the visible frontal part. To fill any gaps and produce

a complete point cloud, multiple images can be acquired by either iteratively moving the camera or the object. This process is time-consuming and introduces new challenges such as the precise matching of the individual point clouds of each view.

To solve this problem, we use a super-quadric representation of objects and reason about symmetry in order to infer the shape of any invisible part. Superquadrics are a family of geometric shapes that can represent a wide range of diverse objects using a limited set of parameters. Superquadrics can be expressed with their implicit equation:

$$\left(\left(\frac{x}{a} \right)^{\frac{2}{\epsilon_2}} + \left(\frac{y}{b} \right)^{\frac{2}{\epsilon_2}} \right)^{\frac{\epsilon_2}{\epsilon_1}} + \left(\frac{z}{c} \right)^{\frac{2}{\epsilon_1}} = 1 \quad (1)$$

In our approach, we generate a super-quadric representation using a single depth image. Fitting of the parameters can be performed online by minimizing the difference between the model and the partial point cloud [11]. However, since only one side of the object is visible, a standard approach to fitting will result in erroneous approximations of the object. To reproduce the entire shape from a partial point cloud, we added an additional pre-processing step to the superquadric fitting process. Instead of using the original point cloud as input, we generate a mirrored version by finding an optimal symmetry plane [11]. The goals of this step is to exploit symmetries to infer invisible parts of an object.

The output of this process for a given object \mathcal{O} consists on a transformation wT_o in world coordinates and the parameters,

$$p_{sq} = \{ a, b, c, \epsilon_1, \epsilon_2 \}$$

defining its approximated geometry. A good number of household objects can be easily described with generic shapes such as boxes, cylinders and ovoids, for which we can further bound the shape parameters considered:

$$\epsilon_1, \epsilon_2 \in [0.1, 1.9]$$

Figure 4 shows different geometric shapes corresponding to superquadrics with different values for ϵ_1 and ϵ_2 .

The superquadric approach turns the pointcloud-based representation into a parametric representation, which can be much more efficiently used during grasp synthesis. Calculations of principal-axes, normals and other features are much faster and less susceptible to noise.

B. Generating Valid Candidates

Once the shape of \mathcal{O} is approximated, we can proceed to generate candidate grasps \mathbf{g}_i using a simulation of the robot, and the object \mathcal{O} , whose mesh is reconstructed by using the superquadric parameters found in the previous section.

The candidates grasps must be kinematically feasible to execute with \mathcal{O} located at both start and goal conditions (wT_s and wT_g). Our approach accomplish this with Algorithm 1. First, we set \mathcal{O} at its goal pose wT_g and generate a set of kinematically feasible grasps for it (\mathcal{G}). Next, we set \mathcal{O} at its start pose wT_s . Finally, we test each of the grasps \mathbf{g}_i from \mathcal{G} in this scenario, discarding the grasps for which there exist

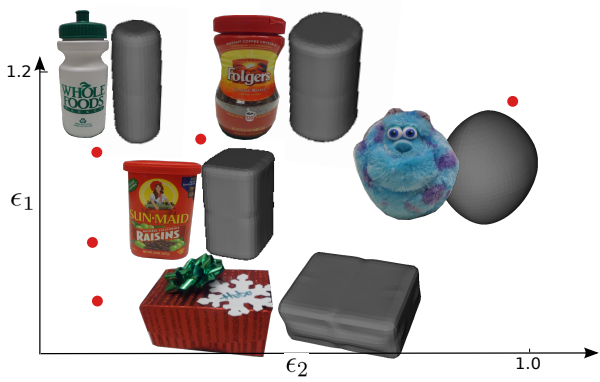


Fig. 4: Examples of superquadrics with different shapes. A variety of shapes can be represented using a small number of parameters.

not a single IK solution. The surviving grasps in \mathcal{G} are then grasps that can be executed for the object \mathcal{O} at both wT_s and wT_g .

Algorithm 1: get_Valid_Candidates

Input: $\mathcal{H}, \mathcal{A}, {}^wT_s, {}^wT_g, \mathcal{O}, p_{sq}$

Output: Set of Candidate grasps \mathcal{G}

```

1 set_Pose( $\mathcal{O}, {}^wT_g$ )
  /* Generate grasps with  $\mathcal{O}$  at  ${}^wT_g$  */
2  $\mathcal{G} \leftarrow$  generate_Grasps( $\mathcal{H}, \mathcal{A}, {}^wT_g, \mathcal{O}, p_{sq}$ )
3 set_Pose( $\mathcal{O}, {}^wT_s$ )
  /* Discard grasps invalid with  $\mathcal{O}$  at  ${}^wT_s$  */
4 foreach  $g_i \in \mathcal{G}$  do
5   if exist_IK_sol( $g_i, \mathcal{H}, \mathcal{A}$ ) is false then
6      $\mathcal{G}.erase(g_i)$ 
7
8 return  $\mathcal{G}$ 

```

1) *Grasp Generation at Goal Pose:* The function generate_Grasps, which we use to produce grasps exploiting the shape parameters of \mathcal{O} is shown in Algorithm 2. First, we uniformly sample the surface of \mathcal{O} . This is easily done by using the explicit equation defining the points in a superquadric and their corresponding normals:

$$\begin{bmatrix} x \\ y \\ z \end{bmatrix} = \begin{bmatrix} a \cos^{\epsilon_1} \eta \cos^{\epsilon_2} \omega \\ b \cos^{\epsilon_1} \eta \sin^{\epsilon_2} \omega \\ c \sin^{\epsilon_1} \eta \end{bmatrix} \quad \text{with} \quad \begin{matrix} \frac{\pi}{2} < \eta < \frac{\pi}{2} \\ \pi < \omega < \pi \end{matrix} \quad (2)$$

$$\begin{bmatrix} n_x \\ n_y \\ n_z \end{bmatrix} = \begin{bmatrix} \frac{1}{a} \cos^{2-\epsilon_1} \eta \cos^{2-\epsilon_2} \omega \\ \frac{1}{b} \cos^{2-\epsilon_1} \eta \sin^{2-\epsilon_2} \omega \\ \frac{1}{c} \sin^{2-\epsilon_1} \eta \end{bmatrix} \quad (3)$$

Sampling uniformly ω and η does not produce a uniform sampling of surface points due to the high nonlinearity of the

superquadrics equation. We use the method proposed by Pilu and Fischer [17] to obtain an evenly-spaced set of points and normals.

To define a grasp we calculate the transformation of the hand \mathcal{H} w.r.t. \mathcal{O} (oT_h). We use the samples to generate this transformation (lines 3 to 7 of Algorithm 2). After positioning the TCP of the \mathcal{H} at wT_p , we close the fingers. If there are not collisions with the environment, we proceed to evaluate if there exists at least an arm configuration that allows the hand to execute the grasp. If so, then a corresponding grasp is stored.

Algorithm 2: GenerateGrasps($\mathcal{H}, \mathcal{A}, {}^wT_o, \mathcal{O}, p_{sq}$)

Input: $\mathcal{H}, \mathcal{A}, {}^wT_o, \mathcal{O}, p_{sq}$

Output: A feasible set of grasps \mathcal{G}

```

/*  $p_{sq} = \{\epsilon_1, \epsilon_2, a, b, c\}$  */
1  $\mathcal{S} =$  sample_SQ( $p_{sq}$ )
2 foreach ( $p_i, n_i$ )  $\in \mathcal{S}$  do
  /*  $p$ : TCP point in the hand  $\mathcal{H}$  */
3    ${}^oT_p.trans = p_i$ 
  /*  $z$ : Approach direction of  $\mathcal{H}$  */
4    ${}^oT_p.z = -n_i$ 
  /*  $x$ : Fingers closing direction */
5    ${}^oT_p.x =$  smallest_Axis( $a, b, c$ )
6    ${}^oT_p.y = {}^oT_h.z \times {}^oT_h.x$ 
7    ${}^wT_p = {}^wT_o \cdot {}^oT_p$ 
  /*  $h$ : Origin of hand  $\mathcal{H}$  */
8    ${}^wT_h = {}^wT_p \cdot {}^pT_h$ 
9   setHand_Tcp( $\mathcal{H}, {}^wT_p$ )
10  close_Hand( $\mathcal{H}$ )
11  if check_collision( $\mathcal{H}$ ) is false then
12    if exist_IK_conf( $\mathcal{H}, \mathcal{A}, {}^wT_h$ ) is true then
13       $\mathcal{G} \leftarrow$  Grasp( $\mathcal{H}, {}^oT_p \cdot {}^pT_h$ )
14
15 return  $\mathcal{G}$ 

```

Algorithm 2 generates at most one grasp per each sampled point. Optionally, we generated 2 additional possible grasps per each point by rotating the hand an angle $\pm\alpha$ around the x axis of oT_p . We added this since we noticed that, when executing the grasps on the physical robot, a slight inclination usually made the grasp much easier to reach. In this paper we used $\alpha = 30^\circ$. An example of the varied grasps generated using α is shown in Figure 5.

2) *Validation at Start Pose:* Once a set of grasps feasible to execute on \mathcal{O} at wT_g is obtained, our algorithm discards the grasps that cannot be executed with \mathcal{O} at wT_s (lines 4 to 6).

V. GRASP PRIORITIZATION

Once a set of feasible grasps \mathcal{G} is generated, paths for reaching and placing the object must be produced. A brute-force approach would be to exhaustively try each grasp in a random

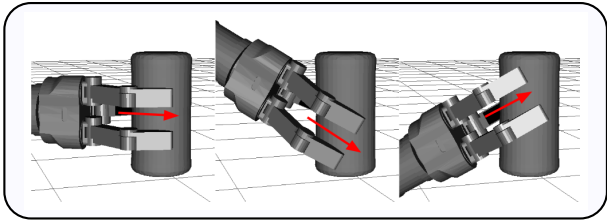


Fig. 5: Generating grasps varying the approach direction by rotating the hand around the local x axis (pointing out the page): Left: Original. Middle, right: After rotating by $\pm\alpha$

order until a solution is found. However, arm planning can be a time-consuming process, particularly when using sampling-based methods. It is therefore desirable to first evaluate grasps that are more likely to produce a solution. Since there is likely more than one solution in \mathcal{G} , it is preferable to choose grasps such that the solution is quickly found. We propose to use *situated grasp manipulability* as a metric to prioritize the grasps and, hence, as a heuristic for guiding the search process.

Manipulability(m) measures how dexterous the end-effector of a robotic arm is at a given joint configuration \mathbf{q} . Initially proposed by Yoshikawa [23], $m(\mathbf{q})$ is defined as:

$$m(\mathbf{q}) = \sqrt{|J(\mathbf{q})J^T(\mathbf{q})|}. \quad (4)$$

Manipulability is typically defined for a single joint configuration. In our scenario, we describe a situated grasp \mathbf{g}_i for which multiple \mathbf{q} might exist, due to redundancy. This naturally leads to the definition of *situated grasp manipulability* (m_g). Given a target object \mathcal{O} located at wT_o , and its corresponding grasp \mathbf{g}_i , we define m_g as the average manipulability of a uniform set of collision-free arm configurations \mathbf{q}_i that allow executing \mathbf{g}_i :

$$m_g = \frac{1}{N} \sum_{i=1}^N m(\mathbf{q}_i) \quad (5)$$

Please note that m_g depends on both \mathbf{g}_i , wT_o and the environment (for collisions) since only collision-free grasps that reach the object are considered. Figure 6 shows an example of a pick-and-place task wherein the green and red markers indicate the wT_s and wT_g . In this case, m_g at wT_g is bigger than wT_s (where $N_s = 76$ and $N_g = 108$ are the number of IK solutions for both situations). When the object is at wT_g , the arm movement requires less effort.

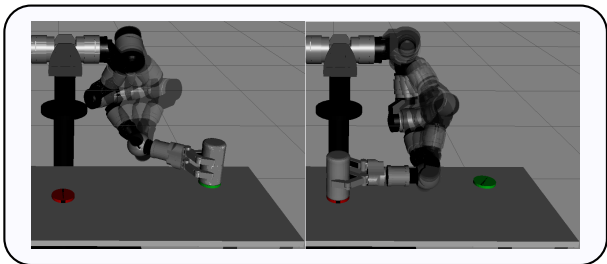


Fig. 6: Examples of m_g measured at wT_s and wT_g

From the shown example, it becomes evident that for a pick-and-place manipulation problem, there are at least two possible metrics to use per grasp \mathbf{g}_i : m_g measured either at wT_s or wT_g . Choosing the first option means that we prioritize grasps in which the pick phase is executed comfortably (wT_s), whereas by choosing the latter, we favor grasps in which the arm configuration used at placing the object (wT_g) is more relaxed. In section VI, we present the results of experiments comparing these two metrics and an additional control measure to analyze their performance and choose which one is best suited for our problem.

VI. EXPERIMENTS AND RESULTS

In this section, we perform a set of experiments in simulation and on the real robot in order to evaluate the introduced manipulation planning algorithm. The simulation experiments are used to analyze the situated grasp manipulability using a large number of trials. Experiments on the real robots are performed to show the generation of manipulations based on task goals and previously unknown objects. Generation of superquadric object models was performed on the spot within 1 second.

A. Simulation Experiments

In this experiment, we consider three alternatives:

- Measure m_g for grasp situated at wT_s
- Measure m_g for grasp situated at wT_g
- Average of both measures above

We use 3 measures to compare the performance of the 3 evaluated metrics.

- *First success*: The main goal of the metrics evaluated is to prioritize the grasps such that the first one tried is the most likely to succeed. This metric indicates the number of times that a solution is found by evaluating only the grasp with the biggest value for the evaluated metric.
- *Planning time*: It measures the average planning time of the succeeding grasps. The planning time is the total time to plan a reach and transport path for the given grasp.
- *Path length*: It indicates the number of steps required for the pick-and-place solution. The step length is a normalized value in joint space, so this metric compare the paths in configuration space.

The scenario we used is depicted in Figure 7. We fix the wT_g to the middle of the table (red marker) and vary the start pose wT_s to 35 positions, each separated 0.1 m (green markers). We devised 2 kind of experiments: In the first, wT_s and wT_g have the same orientation, with only the position being changed (35 scenarios). In the second case, wT_s presents a rotation around the Z axis w.r.t. wT_g in the interval $[0, 2\pi]$ at each $\frac{\pi}{4}$ steps, so in total $35 \times 8 = 280$ scenarios are tested.

We used an standard IK-BiRRT to perform the arm planning. To account for its randomness, the results presented in Table I and Table II are an average of 5 runs per each experiment.

From the tables, we can observe that using m_g evaluated at wT_g produces the best results in terms of success at the first

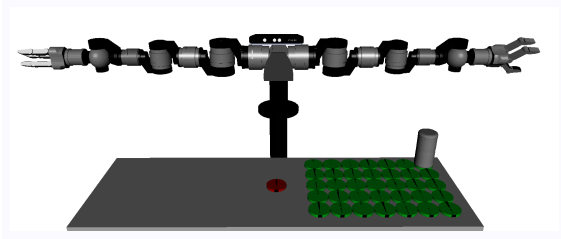


Fig. 7: Setup for unimanual evaluation experiments

TABLE I: Evaluation with no rotation change

Metric Type	Path Steps	Planning Time	Success
m_g at wT_s	82.92	2.17	21.8/35
m_g at wT_g	89.28	2.218	33/35
Avg. m_g	92.92	2.29	31.4/35

trial, whereas wT_s present the worst results. The average path length for the general case of Table II is rather similar for the 3 cases. Regarding planning times, the average m_g gives better results.

Given the results presented, we chose to use the m_g at wT_g . Its next best competitor (the avg. m_g) was not considered since in order to calculate it, the m_g at both wT_s and wT_g must be calculated, which increases the computation time (for the examples presented, the computation time of m_g was 2 seconds). Given that the advantage of planning time is not significant, we chose m_g at wT_g .

B. Robot Experiments

Next, we perform a set of experiments on the real robot. All performed experiments are pick-and-place tasks. However, in some tasks we add environmental constraints at the goal location which limit the range of applicable grasps. Figure 8 depicts two trials without any environmental constraint. The robot has to pick an object at the starting location (green) and move it successfully to the goal location (orange). The robot has no prior knowledge of the object and needs to extract shape information from a single depth image produced by a depth sensor mounted in the head. As can be seen in the figure, the grasp direction and the hand shape is adapted to suit the object.

A different set of experiments can be seen in Figure 9. Here, environmental constraints at the goal are introduced. In the top row, the object has to be placed in a box. Accordingly, the robot has to choose a grasp that allows it to place the object in the box without colliding with it. Hence, the selected grasps are mostly from above. The middle row show a different scenario, in which the object has to be placed on a box which is farther away. Choosing the wrong approach direction, e.g. from above, would prevent the robot from successfully finishing the manipulation process, due to workspace limitations. The bottom row shows normal runs without any environmental constraints.

TABLE II: Evaluation with rotation change

Metric Type	Path Steps	Planning Time	Success
m_g at wT_s	100.7	4.70	255/278
m_g at wT_g	99.6	4.49	275/278
Avg. m_g	100.4	3.83	260/278

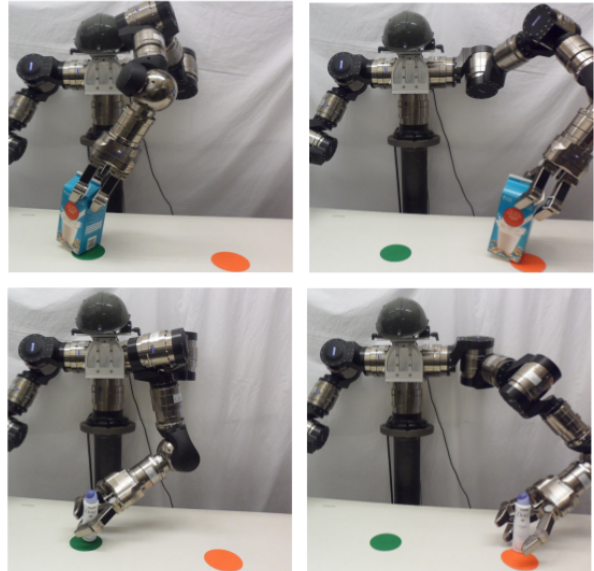


Fig. 8: Two examples of a pick-and-place without constraints. The robot can identify suitable grasp for novel objects using the superquadric representation.

VII. CONCLUSION

In this paper, we introduced a new method for manipulation planning with task constraints. Given a previously unknown object and goals of the task, the method synthesizes online a grasp that facilitates task completion. Planning and grasp synthesis are effectively merged to efficiently produce manipulation sequences. Object acquisition, representation, grasp synthesis and planning can be performed within a couple of seconds, i.e., 2-5 seconds, for the presented examples. We showed how superquadrics and a new heuristic, i.e., the situated grasp manipulability can be used towards this end. These properties, hence, allow a robot to perform successful, goal-driven manipulation tasks in new environments without resorting to prior 3D models of the object or pre-calculated grasps.

While superquadrics can be efficiently calculated, they lack accuracy when representing complex shapes and objects. In this paper, we showed that many objects, in particular household objects can be represented by superquadrics. In our future work, we want to explore extensions of this representation that can model a larger set of objects. In particular, we want to build upon our previous research on the identification of rotational and linear extrusions [11] to represent more complex shapes. In addition, we want to verify the introduced planning approach on longer manipulation sequences.

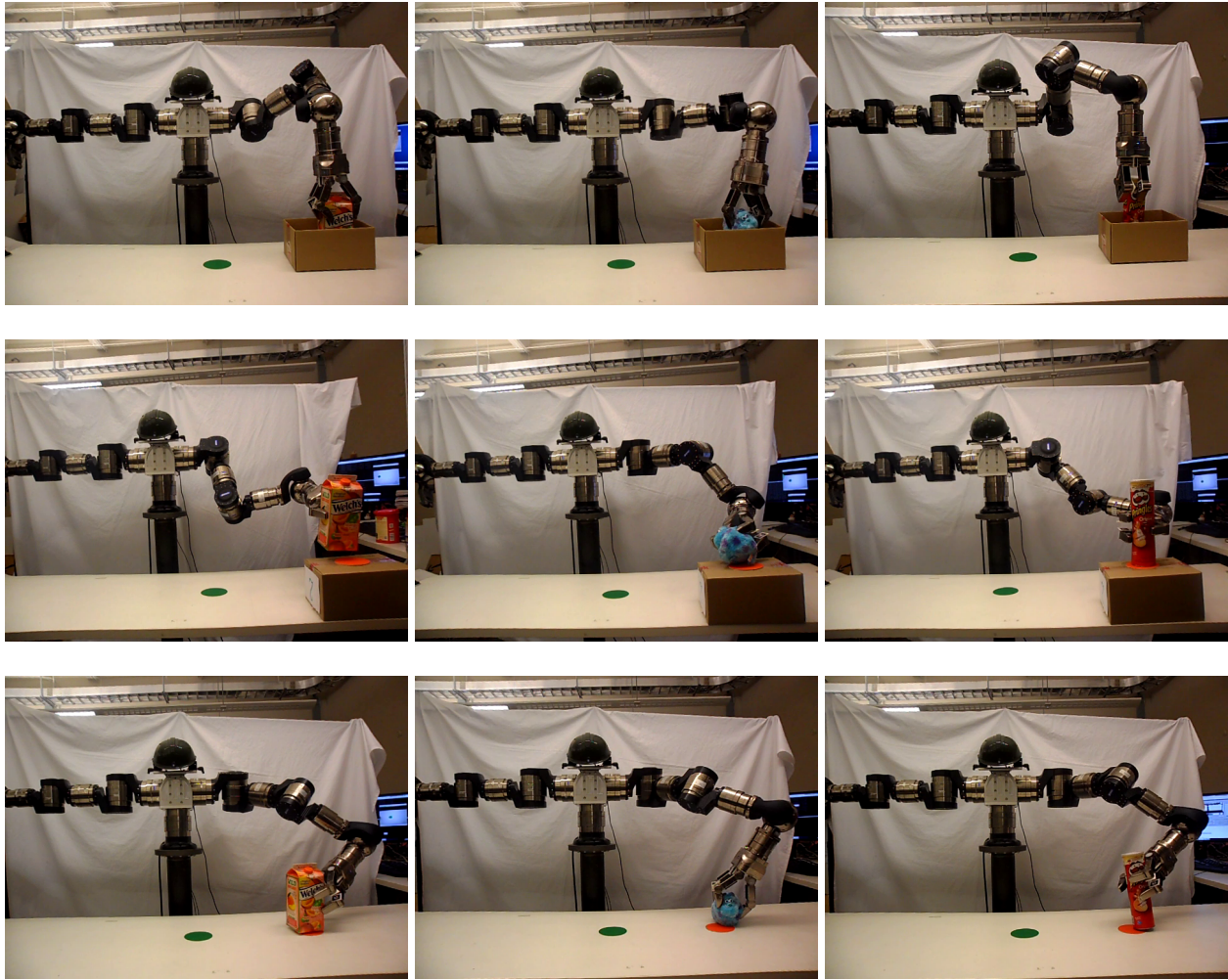


Fig. 9: Final grasp configuration during manipulation with goal constraints (top and middle) and without goal constraints (bottom).

REFERENCES

- [1] R. Balasubramanian, L. Xu, P. D Brook, J.R. Smith, and Y. Matsuoka. Physical human interactive guidance: Identifying grasping principles from human-planned grasps. In *The Human Hand as an Inspiration for Robot Hand Development*. Springer, 2014.
- [2] D. Berenson, R. Diankov, K. Nishiwaki, S. Kagami, and J. Kuffner. Grasp planning in complex scenes. In *7th IEEE-RAS Int. Conf. on Humanoid Robots*, 2007.
- [3] J. Bohg, A. Morales, T. Asfour, and D. Kragic. Data-driven grasp synthesis: A survey. *IEEE Transactions on Robotics*, 2014.
- [4] M. Ciocarlie, C. Goldfeder, and P. Allen. Dimensionality reduction for hand-independent dexterous robotic grasping. In *IEEE/RSJ Int. Conf. on Intelligent Robots and Systems (IROS)*, pages 3270–3275, 2007.
- [5] M.R. Cutkosky. On grasp choice, grasp models, and the design of hands for manufacturing tasks. *IEEE Transactions on Robotics and Automation*, 1989.
- [6] R. Diankov and J. Kuffner. Openrave: A planning architecture for autonomous robotics. *Robotics Institute, Pittsburgh, PA, CMU-RI-TR-08-34*, 79, 2008.
- [7] C. Ferrari and J. Canny. Planning optimal grasps. In *IEEE Int. Conf. on Robotics and Automation (ICRA)*, 1992.
- [8] J. Fontanals, B.A. Dang-Vu, O. Porges, J. Rosell, and M. Roa. Integrated grasp and motion planning using independent contact regions. *14th IEEE-RAS Int. Conf. on Humanoid Robots (Humanoids)*, 2014.
- [9] C. Goldfeder, P.K. Allen, C. Lackner, and R. Pelossof. Grasp planning via decomposition trees. In *IEEE Int. Conf. on Robotics and Automation (ICRA)*, pages 4679–4684, 2007.
- [10] K. Hsiao, S. Chitta, M. T. Ciocarlie, and E. G. Jones. Contact-reactive grasping of objects with partial shape information. In *IEEE/RSJ Int. Conf. on Intelligent Robots and Systems (IROS)*, volume 99, page 124, 2010.
- [11] A. Huamán Quispe, B. Milville, MA. Gutiérrez, C. Erdogan, M. Stilman, HI. Christensen, and H. Ben Amor. Exploiting symmetries and extrusions for grasping household objects. *IEEE Int. Conf. on Robotics and Automation (ICRA)(to appear)*, 2015.
- [12] K. Huebner and D. Kragic. Selection of robot pre-grasps using box-based shape approximation. In *IEEE/RSJ Int. Conf. on Intelligent Robots and Systems (IROS)*, 2008.
- [13] Z. Li and S.S. Sastry. Task-oriented optimal grasping by multifingered robot hands. *IEEE Journal of Robotics and Automation*, 1988.
- [14] J. Loucks and J. A. Sommerville. The role of motor experience in understanding action function: The case of the precision grasp. *Child development*, 83(3):801–809, 2012.
- [15] A.T. Miller, S. Knoop, H.I. Christensen, and P.K. Allen. Automatic grasp planning using shape primitives. In *IEEE Int. Conf. on Robotics and Automation, (ICRA)*, 2003.
- [16] A.K. Pandey, J-P Saut, D. Sidobre, and R. Alami. Towards planning human-robot interactive manipulation tasks: Task dependent and human

- oriented autonomous selection of grasp and placement. In *4th IEEE RAS & EMBS Int. Conf. on Biomedical Robotics and Biomechatronics (BioRob)*, 2012.
- [17] M. Pilu and R.B. Fisher. *Equal-distance sampling of superellipse models*. University of Edinburgh, Department of Artificial Intelligence, 1995.
 - [18] M. Przybylski, T. Asfour, and R. Dillmann. Unions of balls for shape approximation in robot grasping. In *IEEE/RSJ Int. Conf. on Intelligent Robots and Systems (IROS)*, 2010.
 - [19] M. Przybylski, T. Asfour, R. Dillmann, R. Gilster, and H. Deubel. Human-inspired selection of grasp hypotheses for execution on a humanoid robot. In *11th IEEE-RAS Int. Conf. on Humanoid Robots*, 2011.
 - [20] D. A. Rosenbaum, C. M. van Heugten, and G. E. Caldwell. From cognition to biomechanics and back: The end-state comfort effect and the middle-is-faster effect. *Acta psychologica*, 94(1):59–85, 1996.
 - [21] A. Sahbani, S. El-Khoury, and P. Bidaud. An overview of 3d object grasp synthesis algorithms. *Robotics and Autonomous Systems*, 60(3):326–336, 2012.
 - [22] N. Vahrenkamp, T. Asfour, and R. Dillmann. Simultaneous grasp and motion planning: Humanoid robot armar-iii. *Robotics & Automation Magazine*, 2012.
 - [23] T. Yoshikawa. Manipulability of robotic mechanisms. *The International Journal of Robotics Research*, 4(2):3–9, 1985.